ORIGINAL ARTICLE

The expression of YAP1 and other transcription factors contributes to lineage plasticity in combined small cell lung carcinoma

Naoe Jimbo[1]* ![ORCID], Chiho Ohbayashi[2,3], Tomomi Fujii[3], Maiko Takeda[3], Suguru Mitsui[4], Yugo Tanaka[4], Tomoo Itoh[1] and Yoshimasa Maniwa[4]

[1]*Department of Diagnostic Pathology, Kobe University Graduate School of Medicine, Kobe, Japan*
[2]*Department of Diagnostic Pathology, Shinko Hospital, Kobe, Japan*
[3]*Department of Diagnostic Pathology, Nara Medical University, Kashihara, Japan*
[4]*Division of Thoracic Surgery, Kobe University Graduate School of Medicine, Kobe, Japan*

Correspondence to: Naoe Jimbo, Department of Diagnostic Pathology, Kobe University Graduate School of Medicine, 7-5-2 Kusunoki-cho, Chuo-ku, Kobe, Hyogo 650-0017, Japan. E-mail: naoe1123@med.kobe-u.ac.jp

Abstract

Lineage plasticity in small cell lung carcinoma (SCLC) causes therapeutic difficulties. This study aimed to investigate the pathological findings of plasticity in SCLC, focusing on combined SCLC, and elucidate the involvement of YAP1 and other transcription factors. We analysed 100 surgically resected SCLCs through detailed morphological observations and immunohistochemistry for YAP1 and other transcription factors. Component-by-component next-generation sequencing ($n = 15$ pairs) and immunohistochemistry ($n = 35$ pairs) were performed on the combined SCLCs. Compared with pure SCLCs ($n = 65$), combined SCLCs ($n = 35$) showed a significantly larger size, higher expression of NEUROD1, and higher frequency of double-positive transcription factors ($p = 0.0009$, 0.04, and 0.019, respectively). Notably, 34% of the combined SCLCs showed morphological mosaic patterns with unclear boundaries between the SCLC and its partner. Combined SCLCs not only had unique histotypes as partners but also represented different lineage plasticity within the partner. NEUROD1-dominant combined SCLCs had a significantly higher proportion of adenocarcinomas as partners, whereas POU2F3-dominant combined SCLCs had a significantly higher proportion of squamous cell carcinomas as partners ($p = 0.006$ and $p = 0.0006$, respectively). YAP1 expression in SCLC components was found in 80% of combined SCLCs and 62% of pure SCLCs, often showing mosaic-like expression. Among the combined SCLCs with component-specific analysis, the identical *TP53* mutation was found in 10 pairs, and the identical *Rb1* abnormality was found in 2 pairs. On immunohistochemistry, the same abnormal p53 pattern was found in 34 pairs, and Rb1 loss was found in 24 pairs. In conclusion, combined SCLC shows a variety of pathological plasticity. Although combined SCLC is more plastic than pure SCLC, pure SCLC is also a phenotypically plastic tumour. The morphological mosaic pattern and YAP1 mosaic-like expression may represent ongoing lineage plasticity. This study also identified the relationship between transcription factors and partners in combined SCLC. Transcription factors may be involved in differentiating specific cell lineages beyond just 'neuroendocrine'.

Keywords: small cell carcinoma; small cell lung carcinoma; combined small cell lung carcinoma; molecular marker; YAP1; mosaic; transcription factors; plasticity

Introduction

Small cell lung carcinoma (SCLC), in principle, results from the inactivation of the common tumour suppressor genes *TP53* and *Rb1* [1], and has traditionally been considered relatively genetically homogeneous. Rudin

et al reported that SCLCs have been divided into four molecular subtypes (ASCL1, NEUROD1, POU2F3, and YAP1), with heterogeneity at the mRNA level [2]. Each subtype has a different expression profile. For example, ASCL1 and NEUROD1-dominant SCLCs correspond to high-neuroendocrine (NE) and high-TTF-1

phenotypes, while POU2F3 and YAP1-dominant SCLCs usually belong to low-NE and low-TTF-1 phenotypes [3].

Another aspect of SCLC heterogeneity is lineage plasticity between NE and non-NE cells. The transformation of non-SCLC (NSCLC) into SCLC may result from lineage plasticity (which also includes the transformation of SCLC to NSCLC [4]). Lineage plasticity, involving flexible phenotypic changes, favours cancer cell survival under adverse conditions such as hypoxia and driver-targeted therapies [5] and increases the proliferative ability and malignancy of SCLC. Plasticity may be a driving cause of the difficulty in the treatment and poor prognosis of SCLC, making it a hot topic in SCLC research [6].

The question of what pathological findings explain plasticity in SCLC is of significant interest to pathologists; however, limited evidence is available on this subject. Combined SCLC, in which SCLC is combined with a non-SCLC histotype, stands out as a potential target indicating plasticity in SCLC. Component-wise analysis using chromosome studies [7,8] and next-generation sequencing (NGS) [9–12] suggested that combined SCLC forms from a single clone. However, due to its rarity and difficulty in accessing specimens, detailed pathological observations have not been fully conducted.

YAP1 is a downstream effector of the Hippo pathway and is involved in several biological processes such as cell proliferation, migration, and epithelial-mesenchymal transition (EMT) [13,14]. It is upregulated in many human malignancies [15], and its overexpression in NSCLC is considered a poor prognostic factor [16]. In SCLC, YAP1 is involved in cell growth, EMT, drug resistance, and non-NE expression [17,18].

In SCLC, four molecular subtypes have been proposed by Rudin *et al*, including YAP1-dominant SCLC [2], although some reports state that YAP1-expressing SCLC is a cell line-based concept and not applicable to primary SCLC [18,19]. As mentioned above, YAP1 can be considered a non-NE marker in SCLC [17,18] and may be a candidate for plasticity between NE and non-NE types. Furthermore, molecular markers and/or transcription factors may be involved in the development and lineage determination of SCLC, but limited information is available on this.

This study aimed to carry out detailed pathological observations of combined SCLC, focusing on YAP1 and other transcription factors, to approach pathological findings indicating SCLC plasticity.

Materials and methods

Sample and histological examination

This study was approved by the Ethics Committee of Kobe University Hospital (No. B220045) and was conducted in accordance with the Declaration of Helsinki. A total of 100 consecutive cases of surgically resected SCLCs at Kobe University Hospital between 2000 and 2023 and Nara Medical University between 2016 and 2022 were included. Resection methods included total lung resection ($n = 1$), lobectomy ($n = 58$), segmentectomy ($n = 3$), and partial resection ($n = 38$). All patients did not receive pre-operative treatment, such as chemotherapy or radiotherapy. Fifty-three percent of patients received post-operative chemotherapy. Twenty-one patients received carboplatin and etoposide, 11 patients received cisplatin and etoposide, and two patients received cisplatin and irinotecan. Chemotherapy history was unknown for 19 patients.

Two pathologists (NJ and CO) made histopathological diagnoses according to the fifth World Health Organization classification. We evaluated as many H&E slides as possible (average 4.7 tumour-containing slides), because small amounts of NSCLC components were found in some cases. The determination of SCLC or NSCLC was based on H&E, and component amounts were calculated to the nearest 1%. In this study, the partner elements of combined SCLCs included squamous cell carcinoma (SQCC), adenocarcinoma, large-cell neuroendocrine carcinoma (LCNEC), unclassifiable NSCLC, as well as sarcoma, so components other than SCLC are referred to as 'partners'.

Combined SCLCs were classified into the following three morphological patterns: (1) A separated morphological pattern, in which SCLC and partner are separated by clear cell-to-cell boundaries with intervening stroma; (2) a mosaic morphological pattern, in which the cell-to-cell boundary between SCLC and partner is unclear without intervening stroma and they cannot be separated; and (3) coexistence of the two patterns.

Immunohistochemistry

Formalin-fixed paraffin-embedded (FFPE) sections were used for immunohistochemistry (IHC) with a Ventana BenchMark GX (Roche, Switzerland) or BOND-III (Leica, Deer Park, TX, USA) automated immunostainer. Protein expression levels of p53, Rb1, TTF-1, p40, synaptophysin, chromogranin A, CD56, INSM1, ASCL1, NEUROD1, POU2F3, and YAP1 were investigated. The IHC protocols are summarised in supplementary material, Table S1. YAP1

and p40 were assessed on whole slides in all cases, and other antibodies were also assessed on whole slides whenever possible, which was approximately 80% of samples. Cases that could not be studied on whole slides were evaluated using spiral arrays, which are less susceptible to heterogeneity [20]. p40 was used for the purpose of identifying cases containing SQCC and not for statistical analysis. Based on a recent consensus, overexpression, complete absence, and cytoplasmic expression were defined as p53 abnormal patterns [21,22]. Rb1 was classified into two patterns: retained and total loss (>90% loss). For other antibodies, evaluation was performed using the H-score. H-score (0–300) was defined as the product of intensity (0, $1 =$ weak, $2 =$ moderate, and $3 =$ strong) and proportion (0–100%) of the expressed tumour cells, according to a previous study [19,23]. In the combined SCLCs, each component was scored separately, as far as possible. SCLC component scores were used for statistical evaluation.

Among ASCL1, NEUROD1, and POU2F3, the highest expressed marker with an H-score of 50 or more was defined as the dominant transcription subtypes. Cases in which none of the three were expressed above an H-score of 50 were defined as triple-negative (TN). Pure SCLC that predominantly expressed ASCL1, NEUROD1, and POU2F3 were labelled pure SCLC-A, pure SCLC-N, and pure SCLC-P, respectively. Pure SCLC of the TN type was pure SCLC-TN. Combined SCLC-A, SCLC-N, SCLC-P, and SCLC-TN were defined similarly.

Next-generation sequencing

NGS was performed on 17 combined SCLCs. DNA was extracted from an 8-μm-thick FFPE surgical sample using the DNA Isolation Kit for FFPE Tissue Samples (CELLDATE, Fremont, CA, USA). The quality and concentration of the DNA samples were examined using a NanoDrop (Thermo Scientific, Waltham, MA, USA), a 4200 TapeStation, and a Genomic DNA ScreenTape Assay (Agilent Technologies, Santa Clara, CA, USA). Cases with clear boundaries between the SCLC and partner were separated into their respective components by macrodissection. Targeted NGS was performed on MiniSeq (Illumina, Inc., San Diego, CA, USA) using the commercially available gene panel Ampliseq™ for Illumina Cancer Hotspot Ver2 (Illumina, Inc.). This 106-bp-sized gene panel targets 50 cancer-related gene hotspots, including 207 amplicon primers, and can detect single nucleotide variations and indels.

Statistical analyses

Statistical analyses of patient characteristics, prognosis, and IHC results were performed for combined SCLC and pure SCLC. Comparisons of variables for patient characteristics and pathological features were made using Mann–Whitney test or Fisher's exact test. Recurrence-free survival (RFS) was defined as the time from the date of surgery until the date of recurrence or death by any cause. Overall survival (OS) was defined as the time from the date of surgery until death by any cause, or until the last follow-up visit.

RFS and OS were evaluated using the Kaplan–Meier method, and differences in survival curves were assessed using the log-rank test. Statistical analyses of prognosis were performed using EZR version 1.55 (Saitama Medical Center, Jichi Medical University, Saitama, Japan), a graphical user interface of R (The R Foundation for Statistical Computing, Vienna, Austria). For survival analysis, univariate analyses and multivariate analyses adjusted for additional factors were performed [24].

Statistical significance was set at a p value <0.05. All p values were two-sided.

Results

Patient characteristics

As shown in Figure 1A,B, 35 cases were morphologically classified as combined SCLC and 65 as pure SCLC. Of the 100 patients included, 87 were males and 13 were females, with a median age of 72 years (range, 40–91 years). All but one male patient (who had combined SCLC-N) had a history of smoking. The tumour size in the combined SCLC group was significantly larger than that in the pure SCLC group (median 31 versus 25 mm, $p = 0.0009$); however, no significant differences in other factors were observed between the two groups.

IHC

As shown in Figure 1C, NEUROD1 expression was significantly higher in combined SCLCs than in pure SCLCs (median H-score 50 versus 0, $p = 0.04$); however, no significant differences in the expression of other proteins or the composition of dominant transcription types were observed. In 98 cases excluding SCLC-TN, double-positive (H-score ≥ 50) transcription marker cases were significantly more common in combined SCLCs, and single-positive cases were more common in pure SCLCs ($p = 0.019$), suggesting that

A

SCLC (n = 100)
- Combined SCLC (n = 35)
- Pure SCLC (n = 65)

Morphological pattern (Combined SCLC):
- Mosaic (n = 5)
- Separated + Mosaic (n = 7)
- Separated (n = 23)

B

			combined SCLC (n = 35)	pure SCLC (n = 65)	p value
Gender	male	number (%)	31 (89%)	56 (86%)	ns
	female		4 (11%)	9 (14%)	
Age		median (range)	70 (57–89)	73 (40–91)	ns
Smoking		median (pack-year) (range)	55 (0–128)	51 (8–188)	ns
Tumor size		median (mm) (range)	31 (11–68)	25 (8–115)	0.0009 ***
Location	peripheral	number (%)	30 (86%)	46 (71%)	ns
	intermediate/central		5 (14%)	19 (29%)	
Lobe	upper/middle lobe	number (%)	15 (43%)	40 (62%)	ns
	lower		20 (57%)	25 (38%)	
Pathological Stage	1	number (%)	13 (37%)	36 (55%)	ns
	2		13 (37%)	19 (29%)	
	3		6 (17%)	9 (14%)	
	4		3 (9%)	1 (2%)	
Postpostoperative chemotherapy (+)		number (%)	17 (49%)	36 (55%)	ns

C

			combined SCLC (n = 35)	pure SCLC (n = 65)	p value
IHC expression	p53 abonormal pattern umber (%		34 (97%)	65 (100%)	ns
	Rb1 loss umber (%		33 (94%)	59 (91%)	ns
	TTF-1	median H-score (0–300)	240	220	ns
	Synaptophysin		250	250	ns
	ChromograninA		30	10	ns
	CD56		280	290	ns
	INSM1		230	170	ns
	NE-score		195	183	ns
	ASCL1		180	150	ns
	NEUROD1		50	0	0.04*
	POU2F3		0	0	ns
	YAP1		25	5	ns
Dominant transcription type	ASCL1	umber (%	19 (54%)	32 (49%)	ns
	NEUROD1		10 (29%)	12 (18%)	
	POU2F3		5 (14%)	20 (31%)	
	Triple-Negative		1 (3%)	1 (2%)	

E

YAP1 H-score	0	1–99	>100
combined SCLC	7 (20%)	23 (66%)	5 (14%)
pure SCLC	25 (38%)	25 (38%)	15 (23%)

D

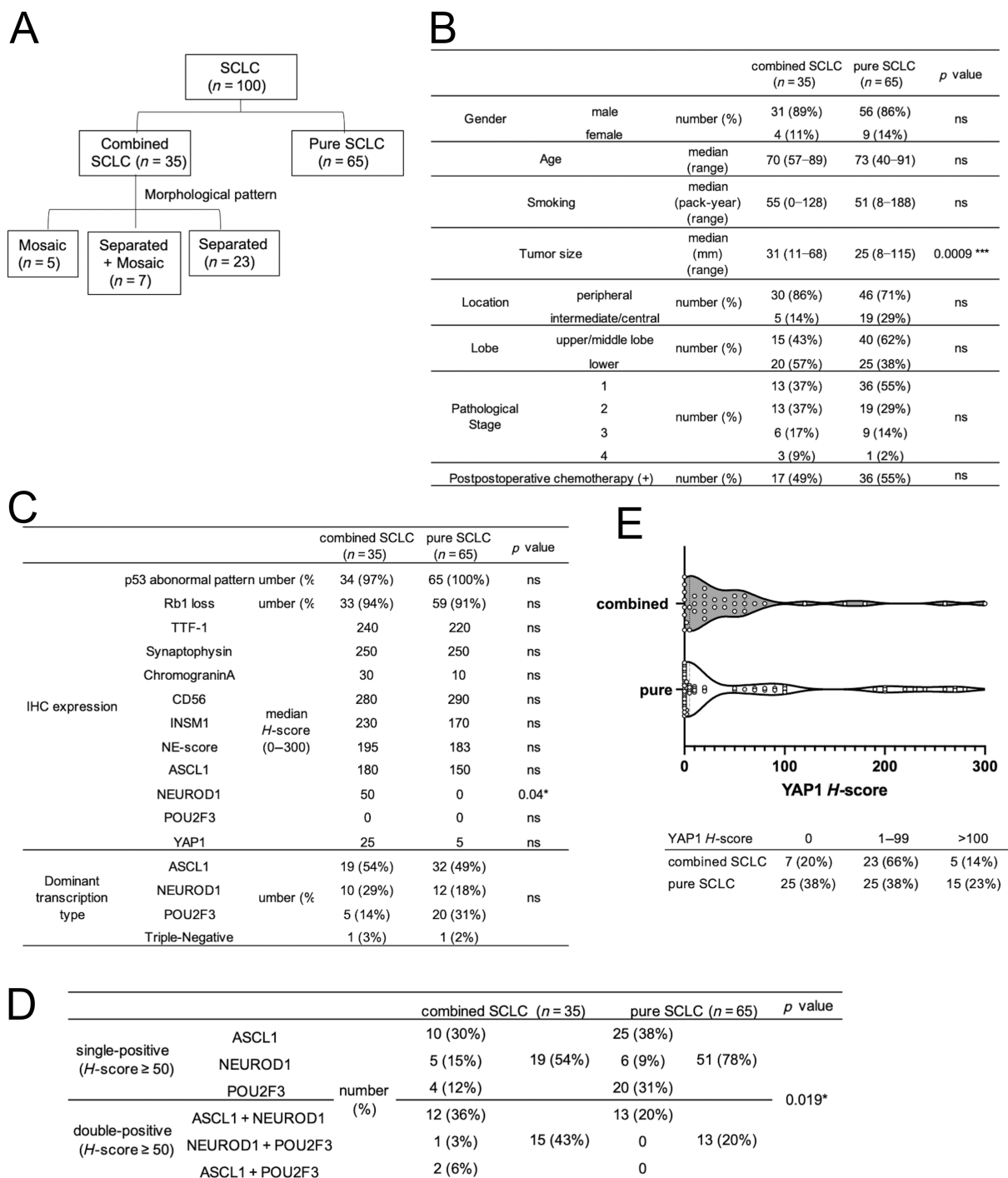|			combined SCLC (n = 35)		pure SCLC (n = 65)		p value
single-positive (H-score ≥ 50)	ASCL1	number (%)	10 (30%)	19 (54%)	25 (38%)	51 (78%)	0.019*
	NEUROD1		5 (15%)		6 (9%)		
	POU2F3		4 (12%)		20 (31%)		
double-positive (H-score ≥ 50)	ASCL1 + NEUROD1		12 (36%)	15 (43%)	13 (20%)	13 (20%)	
	NEUROD1 + POU2F3		1 (3%)		0		
	ASCL1 + POU2F3		2 (6%)		0		

Figure 1. Comparison of clinicopathological findings between combined and pure small cell lung carcinomas. (A) Among 100 cases of small cell lung carcinomas (SCLCs), 35 cases were morphologically classified as combined and 65 as pure SCLCs. (B) Compared with pure SCLCs, combined SCLCs showed a significantly larger size ($p = 0.0009$). (C) Immunohistochemically, combined SCLCs had higher expression of NEUROD1 compared with pure SCLCs ($p = 0.04$), with no significant differences in other protein expression or composition of dominant transcription subtypes. (D) Double-positive transcription factors expression was significantly more common in combined SCLCs, and single marker positivity was more common in pure SCLCs ($p = 0.019$). (E) Distribution of YAP1 expression (H-score) of SCLC components in combined SCLCs and pure SCLCs. YAP1 expression (H-score > 1) was found in 80% of combined SCLCs and 62% of pure SCLCs.

combined SCLCs have stronger plasticity between transcription marker expression (Figure 1D).

YAP1 expression

Figure 1E shows the distribution of YAP1 expression (*H*-score) in the SCLC components of combined and pure SCLCs. YAP1 expression (*H*-score > 1) was observed in 80% of combined SCLCs and 62% of pure SCLCs. The YAP1-negative rate in SCLC components was 20% for combined SCLCs and 38% for pure SCLCs.

Prognosis

In univariate and multivariate analyses for OS, the presence of chemotherapy was a significant favourable prognostic factor, and the presence of interstitial pneumonia was a significant unfavourable prognostic factor (Table 1). Combined SCLCs tended to have a poorer prognosis than pure SCLCs regarding OS, but this was not significant (Table 1).

Pathological features of combined SCLCs

Thirty-five combined SCLCs were morphologically classified as mosaic type (5 cases), coexisting mosaic and separated type (7 cases), or separated type (23 cases) (Figures 1A and 2A). The median proportions of SCLC components in the total tumours of each type were 90%, 70%, and 40%, respectively (Figure 2B). The proportion of SCLC in the total tumour was significantly lower in the separated morphological pattern than in the other two patterns ($p = 0.018$).

In separated morphological patterns, clear boundaries existed between SCLC and the partner (Figure 3A,B), which were also highlighted by NEUROD1 and Napsin A (Figure 3A) or POU2F3 and p40 (Figure 3B). At high magnification, SCLC and its partners were accompanied by clear intervening stromal components, which could be seen in YAP1 expression. YAP1 was focally expressed in areas of morphological SCLC (data not shown).

In the mosaic morphological pattern, partners (all of which were NSCLC of this type) were scattered in a mosaic-like pattern. Indistinct and ambiguous boundaries were observed between the SCLC and NSCLC partners without intervening stroma. YAP1 showed mosaic-like expression, almost coinciding with areas that were morphologically NSCLC, but was also weakly expressed in areas that were morphologically SCLC (Figure 3C,D). The border between SCLC and NSCLC was ambiguous in both H&E and YAP1 cells, indicating a gradual transition between SCLC and NSCLC. In the adenocarcinoma components of combined SCLC showing mosaic morphological types,

Table 1. Univariable and multivariable analyses of covariables associated with recurrence-free survival and overall survival

	Univariate			Multivariate		
	HR	95% CI	*p* value	HR	95% CI	*p* value
Outcomes (recurrence-free survival)						
Age (≤70 versus >70)	1.4320	0.7231–2.8360	0.3030	1.4110	0.6763–2.9430	0.3590
Surgical procedure (lobotomy or more versus sublobar resection)	1.1450	0.5628–2.3300	0.7086	1.1320	0.4928–2.6000	0.7703
Chemotherapy (chemotherapy-treated versus non-treated)	0.7279	0.3780–1.4020	0.3420	0.5623	0.2611–1.2110	0.1413
Comorbidities (IP versus non-IP)	1.8830	0.9041–3.9210	0.0909	2.0230	0.8975–4.5580	0.0893
Tumour size (≤20 versus >20)	0.4717	0.1832–1.2140	0.1190	0.5126	0.1835–1.4320	0.2024
Histology (Pure SCLC versus Combined SCLC)	0.6908	0.3451–1.3830	0.2963	0.9431	0.4344–2.0480	0.8823
Sex (male versus female)	0.9527	0.3364–2.6980	0.9273			
YAP (0 versus *H*-score ≥ 1)	0.9263	0.4687–1.8310	0.8257			
Outcomes (overall survival)						
Age (≤70 versus >70)	1.2330	0.6271–2.4250	0.5436	1.3550	0.6425–2.8580	0.4249
Surgical procedure (lobotomy or more versus sublobar resection)	0.7491	0.3848–1.4580	0.3955	0.9263	0.4153–2.0660	0.8516
Chemotherapy (chemotherapy-treated versus non-treated)	0.4736	0.2449–0.9157	0.0263*	0.3524	0.1585–0.7835	0.0105*
Comorbidities (IP versus non-IP)	2.4640	1.2170–4.9850	0.0122*	2.4300	1.0700–5.5190	0.0339*
Tumour size (≤20 versus >20)	0.6126	0.2553–1.4700	0.2725	0.6312	0.2300–1.7320	0.3717
Histology (pure SCLC versus combined SCLC)	0.5510	0.2841–1.0690	0.0779	0.6571	0.2953–1.4620	0.3034
Sex (male versus female)	0.5566	0.2307–1.3430	0.1924			
YAP (0 versus *H*-score ≥ 1)	0.9425	0.4831–1.8390	0.8622			

In univariate and multivariate analyses for overall survival, the presence of chemotherapy was a significant favourable prognostic factor, and the presence of interstitial pneumonia was a significant unfavourable prognostic factor. Combined SCLCs tended to have a poorer prognosis than pure SCLCs regarding overall survival, but this was not significant.
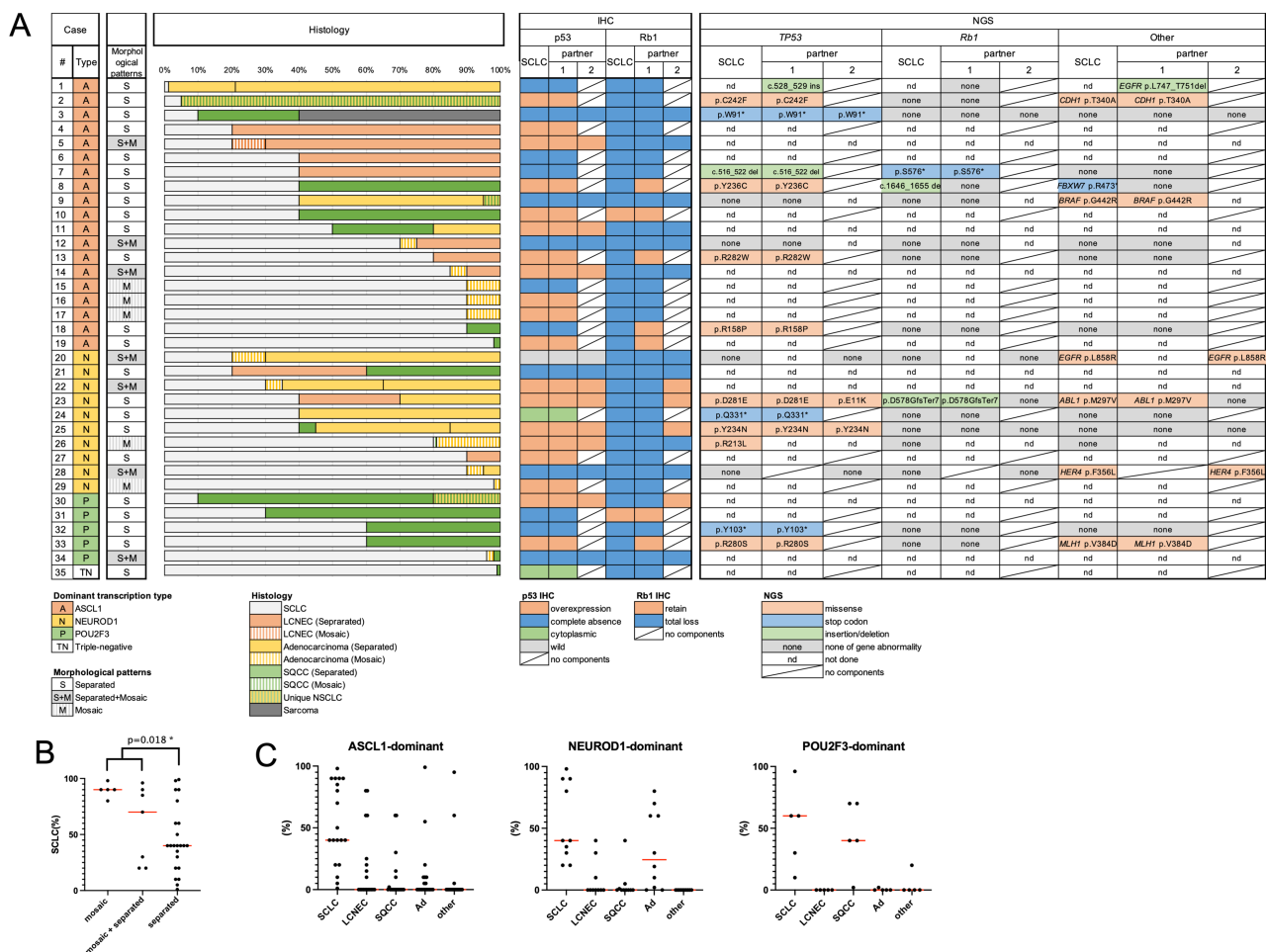*Significant *p* values (*p* < 0.05).

Figure 2. Results of combined small cell lung carcinomas. (A) Summary of results in 35 cases of combined small cell lung carcinoma (SCLC), including dominant transcription subtype, morphological patterns, histopathology details, immunohistochemistry for p53 and Rb1, and genomic analysis. (B) The proportion of SCLC in the total tumour was higher in the order of mosaic, mixture of mosaic and separated, and separated types. A significant difference in the proportion of SCLC was observed between the first two types and the separated type ($p = 0.019$). (C) The proportion of partner histotype in the total tumour depends on the dominant transcription subtype. As partners, NEUROD1-dominant combined SCLCs had a significantly higher proportion of adenocarcinoma ($p = 0.006$), and POU2F3-dominant combined SCLCs had a significantly higher proportion of squamous cell carcinoma ($p = 0.0006$). The red lines indicate the median values.

Rb1 was lost, as in SCLC components (arrows in Figure 3C,D).

Pathological features of pure SCLCs focusing on YAP1 expression

All pure SCLCs exhibited homogeneous small-cell cytology. Figure 4 shows four representative examples of ASCL1-dominant pure SCLCs. In YAP1-negative cases, YAP1 was completely negative, and ASCL1 was positive (Figure 4A). In cases with a YAP1 H-score of 1–99, YAP1 was expressed in a mosaic pattern with a mutually exclusive expression pattern with ASCL1 (Figure 4B,C). In cases with a YAP1 H-score

of 100 or more, both YAP1 and ASCL1 were usually diffusely positive (Figure 4D). Importantly, YAP1 was expressed with a uniform small-cell morphology. Based on the assumption that YAP1 is a non-NE marker [17,18], this suggests a mixture of NE and non-NE phenotypes, even in morphologically homogeneous SCLC. In YAP1-positive cases of pure SCLCs, YAP1 was expressed mostly in a mosaic-like pattern, similar to YAP1 mosaic-like expression in combined SCLCs.

Partners in the combined SCLCs

As shown in Figure 2A, most of the combined SCLCs had classical LCNEC, SQCC, and adenocarcinoma
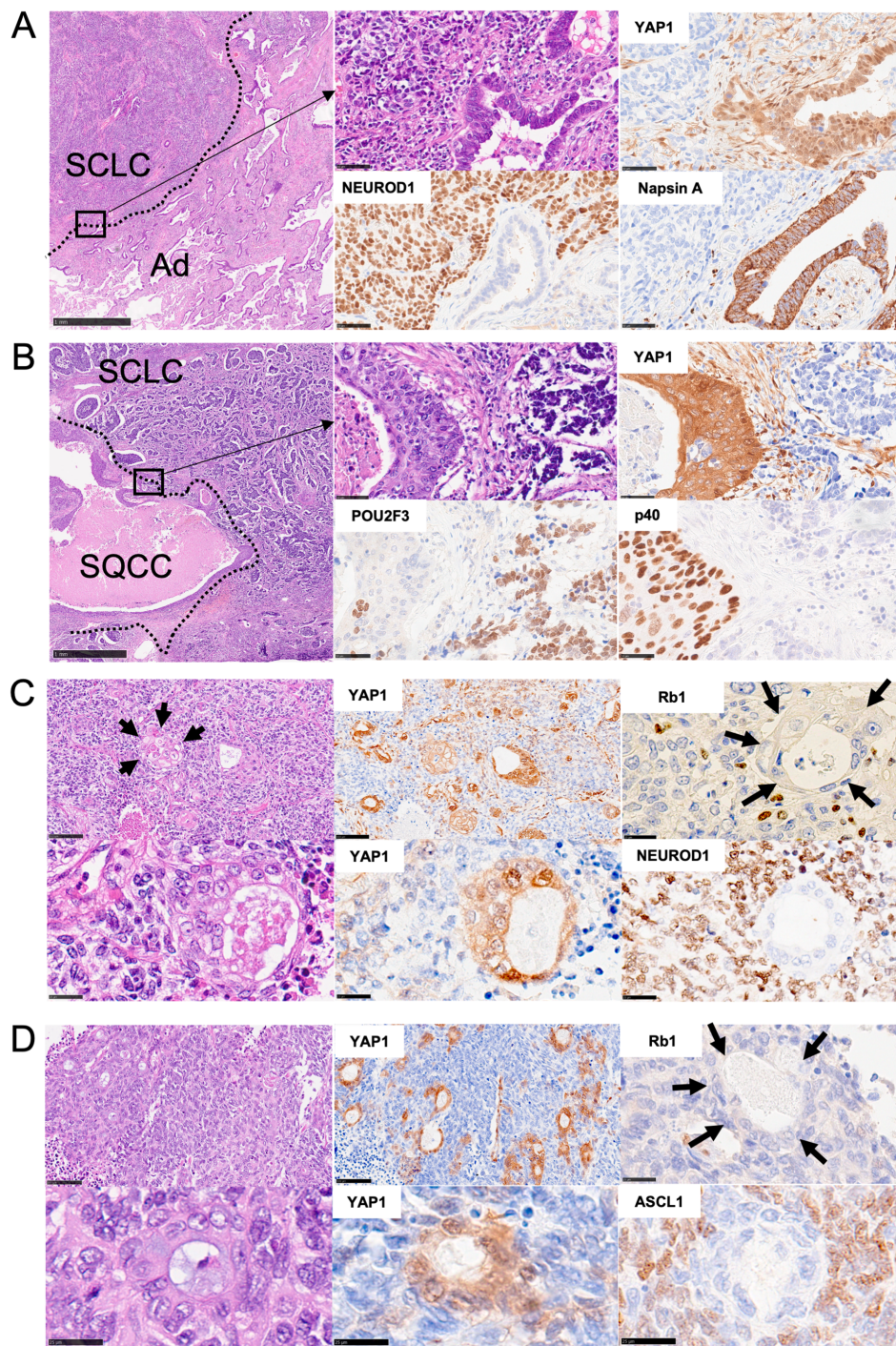
Figure 3. Representative pathological findings in combined small cell lung carcinomas. (A, B) In the separated morphological type, small cell lung carcinoma (SCLC) and each partner were distributed with a clear boundary. At high magnification, they were accompanied by intervening stromal components, which could also be seen in the YAP1 immunostain. (C, D) The boundaries between the SCLC and each partner were indistinct in the mosaic morphological types, and the partners were scattered and mosaic-like. Foci of squamous cell carcinoma are seen in C (arrows). The distribution of the mosaic-like pattern was clearly visible in the YAP1 immunostain. High magnification shows direct contact between the SCLC and the partner, with little or no intervening interstitial components, which was also observed with YAP1. In the adenocarcinoma components of combined SCLC showing mosaic morphological types, Rb1 was lost, as in SCLC components (arrows in C and D).
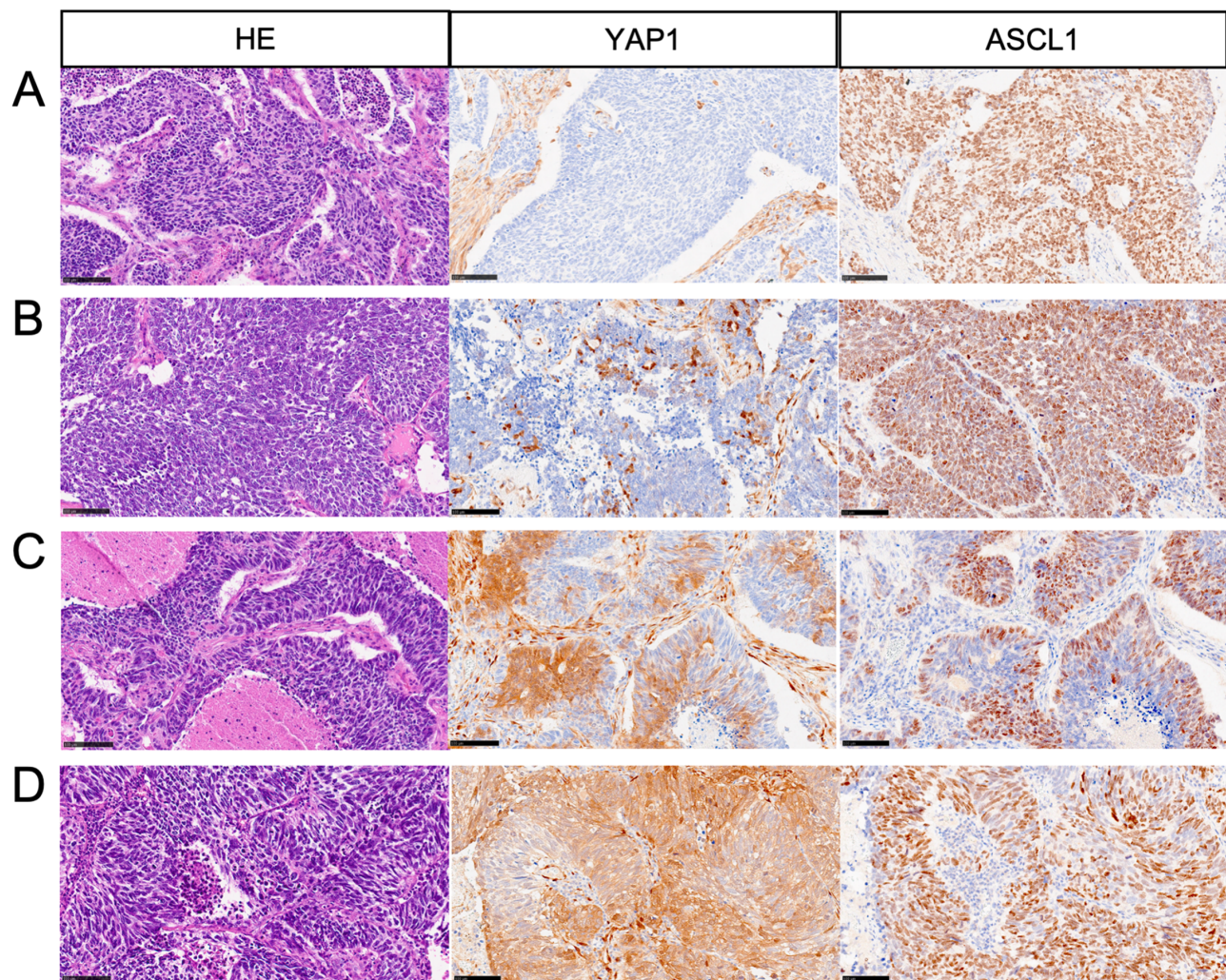
Figure 4. Results of pure small cell lung carcinomas with a focus on YAP1 expression. YAP1 expression pattern in ASCL1-dominant pure small cell lung carcinomas (SCLCs). (A) YAP1 is completely negative for SCLC and diffusely positive for ASCL1. (B, C) YAP1 is partial and mosaic-like positive for SCLC, and ASCL1 was almost complementary to YAP1 expression. (D) ASCL1 and YAP1 are diffusely positive.

as partners. The number of partners in combined SCLC was not always one, with 37% (13/35) of combined SCLC cases having a third partner and three cases of combined SCLC having both well- and poorly differentiated adenocarcinomas as partners (cases #1, 22, and 25). As a unique partner, one case (case #30) had mixed adenocarcinoma and SQCC, showing a biphasic pattern with p40-positive SQCC in the outer layer and adenocarcinoma in the inner layer, similar to tumours recognised as mucoepidermoid carcinoma-like adenosquamous carcinoma in a previous study [25] (Figure 5A). Two patients (cases #2 and 9) had NSCLC that could not be determined histopathologically or phenotypically, with a mixed expression of TTF-1 and p40 by double IHC (Figure 5B). One case (case #3)

included myogenin-positive rhabdomyosarcoma in addition to SQCC (Figure 5C). The presence of these lineage varieties as partners in combined SCLC suggests that other plasticities occur simultaneously (between adenocarcinoma and SQCC or carcinoma and sarcoma), along with lineage plasticity between NE and non-NE components.

Characteristics of partners in combined SCLCs by dominant transcription subtypes

Among the combined SCLCs, the area occupied by SCLC varied from 1% to 99% (median, 40%). No significant differences were observed in the areas occupied by SCLC among the three dominant
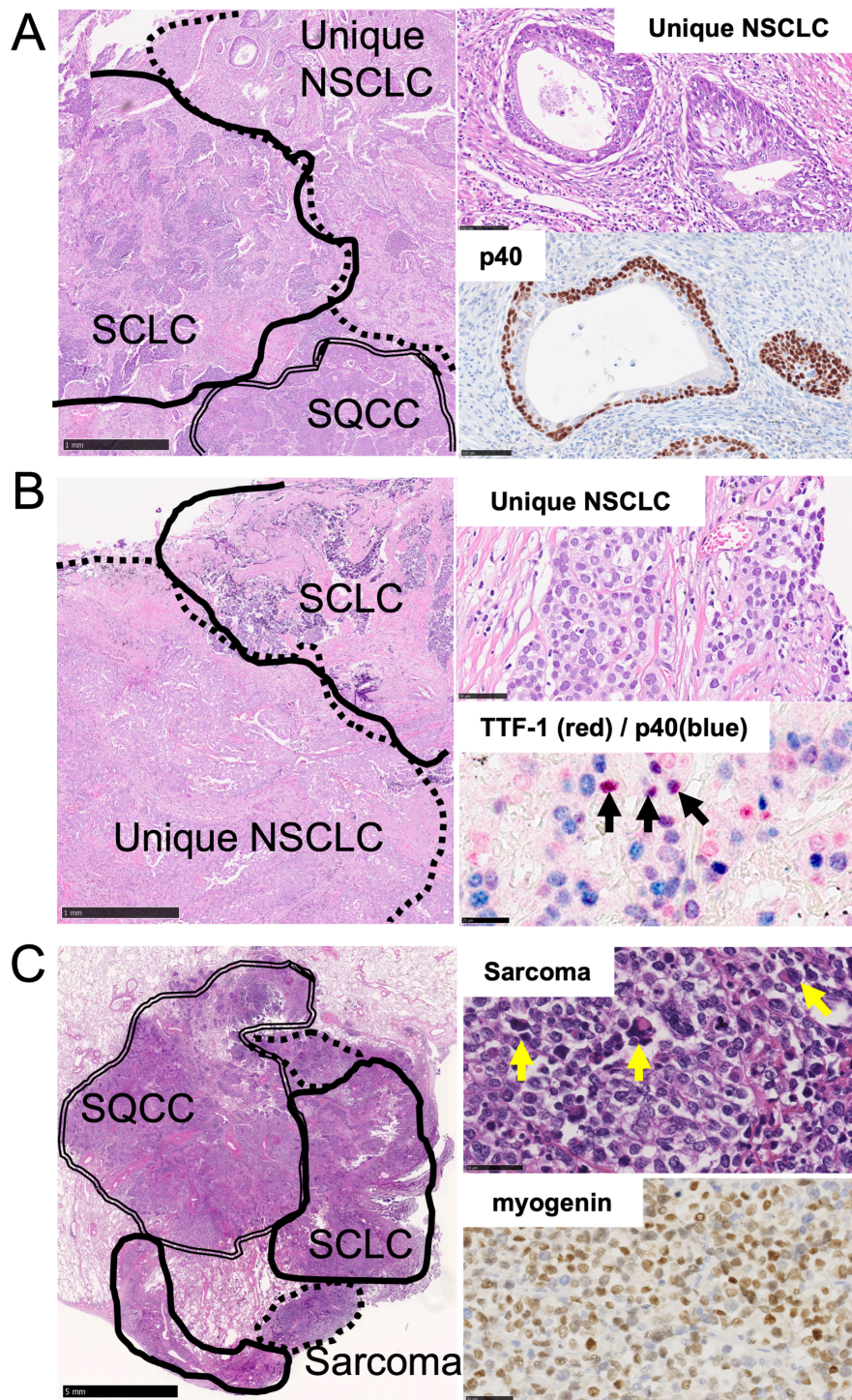
Figure 5. Unique partners in combined small cell lung carcinomas. (A) In the upper case, apart from conventional squamous cell carcinoma (SQCC), a mixed adenocarcinoma (Ad) and SQCC are observed (*), showing a biphasic pattern with p40-positive SQCC in the outer layer and adenocarcinoma in the inner layer. This resembles a tumour recognised as a mucoepidermoid carcinoma-like adenosquamous carcinoma. (B) The second case contains a non-small cell carcinoma component that could not be morphologically and phenotypically determined as adenocarcinoma or SQCC and showed mixed expression of TTF-1 (red) and p40 (blue) by double immunohistochemistry. Black-coloured arrows indicate double-positive cells. (C) The third case had a rhabdomyosarcoma component that was positive for myogenin. Yellow-coloured arrows indicate rhabdoid cells.

transcription subtypes. Interestingly, a relationship was found between dominant transcription subtype and NSCLC partners. The adenocarcinoma area in the combined SCLC-N group was significantly larger than that in the combined SCLC group (median rate, 25% versus 0%, $p = 0.006$). Conversely, the SQCC area in the combined SCLC-P group was significantly larger than that in the combined SCLC group (median rate 40% versus 0%, $p = 0.0006$). Figure 2A,C also indicates that adenocarcinoma was abundant in combined SCLC-N, while SQCC dominates in combined SCLC-P. In contrast, SCLC-A was a mix of different NSCLC partners with no discernible trend.

Concordance of p53 and Rb1 IHC by each component in the combined SCLCs

The expressions of p53 and Rb1 were assessed in each component, including the partner, in mosaic patterns, with 85 samples assessed in all 35 cases. p53 showed almost universal abnormal expression in both SCLC and partner (97%; Figure 2A), with only three components of one combined SCLC showing wild-type p53 (case #20). Rb1 loss was found in 94% (33 of 35) of SCLC and 78% (39 of 50) of the partners. The p53 and Rb1 aberration concordance rates for all partners showing the same aberrant expression as in SCLC were 100% (34/34) and 72% (24/33), respectively. Discordant Rb1 aberration patterns were observed in nine cases, where all components of SCLC showed loss of Rb1, while one or more of the partners showed retention of Rb1. All cases showing discordant Rb1 expression were of a separated morphological type (Figure 2A).

NGS in combined SCLC

A total of 35 DNA samples from 17 patients were examined using NGS. Among the 15 pairs of combined SCLCs in which component-by-component analysis was possible, *TP53* abnormalities were found in 73% (11/15) and *Rb1* abnormalities were identified in 20% (3/15). The *TP53* and *Rb1* aberration concordance rates for all partners with the identical aberration as SCLC were 91% (10/11) and 66% (2/3), respectively. In one case (case #23), the site of the *TP53* mutation differed between NEC (SCLC and LCNEC) and adenocarcinoma. In case #8, only the SCLC had the *Rb1* deletion and *FBXW7* mutation, although both the SCLC and SQCC shared the same *TP53* missense mutation. *EGFR* mutations were observed in two cases: one was confirmed in both SCLC and adenocarcinoma (case #20; this patient was the only non-smoker).

Other mutations, such as *CDH1, BRAF, ABL1, HER4,* and *MLH1*, resulted in the same mutation spots in both SCLC and its partner. The variant allele frequency was generally higher in SCLC than in the partners, possibly due to the hypercellularity of SCLC.

Discussion

In our study, the prevalence of combined SCLCs in resected SCLCs was 35%, whereas previous reports have ranged from 5% to 34% [11,12,20,26]. These discrepancies may stem from variations in the thoroughness of efforts to differentiate between SCLC and NSCLC, requiring cautious interpretation of the results. However, we believe our results are accurate because we performed a careful pathological and morphological evaluation. The tumour size of combined SCLCs was significantly larger than that of pure SCLCs. The presence of NSCLC components with lower proliferative activity may lead to clinical recognition after the tumour has become larger.

Detailed morphological observations further highlighted the morphological variations in the combined SCLCs. Notably, in one-third of the combined SCLC cases, partners were distributed in a mosaic pattern, with five cases consisting of only this mosaic pattern. Combined SCLCs with a mosaic pattern had no obvious intervening stroma between the SCLC and partner. This mosaic morphological pattern appears to indicate the presence of a transitional capacity between SCLC and its partner and may be a pathological finding indicative of SCLC plasticity.

Another interesting phenomenon was the identification of unique plasticity between partners, such as carcinoma and sarcoma, or adenocarcinoma and SQCC. Furthermore, two cases of combined SCLCs had NSCLC partners that could not be classified as adenocarcinoma or SQCC. Recently, TTF1/p40 diffuse double-positive NSCLC showing bilineage differentiation at the same cellular level, which may be due to progenitor cell plasticity, has been reported [27–29]. Plasticity between adenocarcinoma-SQCCs has been reported to be involved in treatment resistance [30]. Combined SCLC may resist adverse conditions by exhibiting a variety of plasticity.

YAP1 expression was found not only in NSCLC partners but also in SCLC components in 80% of combined SCLCs and 62% of pure SCLCs, with most showing a mosaic pattern. Similar mosaic-like YAP1 expression has already been suggested in several reports [19,31]. Importantly, YAP1 was expressed in

SCLC components with uniform small-cell morphology, whether combined or pure. Based on the assumption that YAP1 is a non-NE marker [17,18], this suggests a mixture of NE and non-NE phenotypes, even in morphological SCLC. The YAP1 mosaic pattern appeared to symbolise fluctuations between SCLC (NE) and the partner (non-NE), even in morphological SCLC. YAP1 mosaic-like expression was found in both combined and pure SCLC. Combined SCLC is a more morphologically and phenotypically complex tumour than pure SCLC; however, pure SCLC is also a phenotypically complex tumour with various YAP1 patterns, including mosaic-like expression. If so, mosaic-like YAP1 expression in pure SCLC may represent phenotypic plasticity and be reminiscent of latent combined SCLC, implying a sequential pathogenesis between combined and pure SCLC.

Combined SCLC had significantly higher expression of NEUROD1, and significantly more cases were double-positive for the transcription markers than pure SCLC. Recent reports have shown a high proportion of the NEUROD1-dominant type in combined SCLC [31], suggesting some influence of transcription markers, especially NEUROD1, on the development of combined SCLC.

As another novel insight, an association was found between transcription subtypes and types of partner in combined SCLC. Combined SCLC-A had various NSCLC as partners, while combined SCLC-N had a significantly higher proportion of adenocarcinoma components, and combined SCLC-P had a significantly higher proportion of SQCC components. NEUROD1 participates in the formation of alveolar septa and NE differentiation [32], while POU2F3 is involved in the generation of tuft cells in close association with basal cells [33]. These findings could also provide evidence supporting the relationship between transcription markers and NSCLC partners in combined SCLC.

The cellular origin of SCLC has been postulated to be NE cells or NE stem cells [5,34], and studies using mouse models have demonstrated that SCLC arises most efficiently from NE cells but also from a subset of alveolar type 2 cells and basal cells [35,36]. SCLC is also highly plastic and can assume entirely different NE and non-NE fates via NOTCH signals [37]. Although de novo SCLC can certainly occur, as supported by in situ SCLC [38], it is also believed that a significant number of SCLC are of epithelial rather than NE origin, reflecting epithelial-NE conversion in advanced cases [5,39].

In this study, component-wise NGS (for 15 pairs of combined SCLCs) and IHC (for 35 pairs) were performed. By NGS, 10 pairs of combined SCLCs had the identical TP53 mutation, and two pairs had the identical Rb1 abnormality. On IHC, 34 pairs of combined SCLCs exhibited the same abnormal p53 pattern, while 24 pairs showed Rb1 loss. The rate of positive abnormalities in NGS is low due to panel sequencing, and the number of NGS cases is limited. Although strictly proving clonality may be challenging, the presence of the identical TP53 mutation in 10 pairs supports the single clone theory of combined SCLC. Combined SCLC is a symbolic morphological finding of plasticity between NE and non-NE. It is difficult to determine the direction of tumour differentiation; however, the presence of a certain number of cases with Rb1/Rb1 abnormalities only in SCLC provides evidence for the possibility that SCLC abnormalities occur in the order TP53/p53 to Rb1/Rb1 and the possibility that conversion occurs from NSCLC to SCLC.

The current standard treatment for all SCLC needs to be reexamined to determine the best therapy. Similar treatment strategies have been recommended for both combined and pure SCLC. However, responses to tyrosine kinase inhibitors (TKIs) in EGFR-mutant SCLC have been reported [40], and EGFR-TKIs may be an option, especially in cases with a high proportion of EGFR-mutant NSCLC. In combined SCLC, it has been reported that different partners have different vulnerabilities to certain cell death pathways, such as ferroptosis [41], which may provide a basis for suggesting different treatment strategies depending on the type of partner and also strengthen the relationship between partner and molecular and/or transcription-based classification.

The limitations of this study include selection bias due to limited surgical material. Surgical materials must be selected for detailed observation; however, studies using small samples, including biopsies, need to verify this in the future. A second limitation was the impact of block quality, as older blocks may have decreased immunosignal intensity. The median H-score was higher in the most recent FFPE blocks than in the oldest ones for the antibodies stained in the nucleus, but not significantly different (pathological images from old and recent FFPE blocks are shown in supplementary material, Figure S1). The use of FFPE blocks that are too old should be avoided but, given the limited number of surgical SCLC cases, these had to be used in this study. At our institution, more attention has been paid to fixation and quality control since 2000, which may minimise the effects of age-related degeneration. The third limitation of NGS in this study was the hotspot analysis and exon sequencing. For rigorous proof of

clonality, it may be necessary to analyse genomic tests with higher coverage.

In conclusion, combined SCLC is a more morphologically and phenotypically complex tumour compared with pure SCLC. However, pure SCLC is a phenotypically complex tumour in terms of YAP1 expression. The morphological mosaic pattern and YAP1 mosaic-like expression may help to visualise the ongoing lineage plasticity. Another point is that NSCLC partners in combined SCLC were differentially characterised by transcription marker expression, with NEUROD1 showing high affinity for adenocarcinoma and POU2F3 for SQCC. These results suggest that transcription factors are involved in specific cell lineages and not only in NE cells.

Acknowledgements

Author contributions statement

NJ and CO contributed to the conception, study design, interpretation and drafting of the manuscript. TF and MT contributed to sample collection, genetic analysis and revision of the manuscript. SM, YT and YM provided the samples, performed prognostic analysis and revised the manuscript. TI contributed to the IHC and revised the manuscript. All the authors approved the final version of the manuscript.

Data availability statement

The data that support the findings of this study are available from the corresponding author upon reasonable request.

References

1. George J, Lim JS, Jang SJ, *et al*. Comprehensive genomic profiles of small cell lung cancer. *Nature* 2015; **524**: 47–53.

2. Rudin CM, Poirier JT, Byers LA, *et al*. Molecular subtypes of small cell lung cancer: a synthesis of human and mouse model data. *Nat Rev Cancer* 2019; **19**: 289–297.

3. Lantuejoul S, Fernandez-Cuesta L, Damiola F, *et al*. New molecular classification of large cell neuroendocrine carcinoma and small cell lung carcinoma with potential therapeutic impacts. *Transl Lung Cancer Res* 2020; **9**: 2233–2244.

4. Watanabe K, Kage H, Shinozaki-Ushiku A, *et al*. Spontaneous transdifferentiation from small cell lung carcinoma to squamous cell carcinoma. *J Thorac Oncol* 2019; **14**: e31–e34.

5. Quintanal-Villalonga A, Chan JM, Yu HA, *et al*. Lineage plasticity in cancer: a shared pathway of therapeutic resistance. *Nat Rev Clin Oncol* 2020; **17**: 360–371.

6. Rubin MA, Bristow RG, Thienger PD, *et al*. Impact of lineage plasticity to and from a neuroendocrine phenotype on progression and response in prostate and lung cancers. *Mol Cell* 2020; **80**: 562–577.

7. Murase T, Takino H, Shimizu S, *et al*. Clonality analysis of different histological components in combined small cell and non-small cell carcinoma of the lung. *Hum Pathol* 2003; **34**: 1178–1184.

8. Wagner PL, Kitabayashi N, Chen YT, *et al*. Combined small cell lung carcinomas: genotypic and immunophenotypic analysis of the separate morphologic components. *Am J Clin Pathol* 2009; **131**: 376–382.

9. Quintanal-Villalonga A, Taniguchi H, Zhan YA, *et al*. Multiomic analysis of lung tumors defines pathways activated in neuroendocrine transformation. *Cancer Discov* 2021; **11**: 3028–3047.

10. Lin MW, Su KY, Su TJ, *et al*. Clinic pathological and genomic comparisons between different histologic components in combined small cell lung cancer and non-small cell lung cancer. *Lung Cancer* 2018; **125**: 282–290.

11. Zhao X, McCutcheon JN, Kallakury B, *et al*. Combined small cell carcinoma of the lung: is it a single entity? *J Thorac Oncol* 2018; **13**: 237–245.

12. Zhang J, Zhang L, Luo J, *et al*. Comprehensive genomic profiling of combined small cell lung cancer. *Transl Lung Cancer Res* 2021; **10**: 636–650.

13. Yu FX, Zhao B, Guan KL. Hippo pathway in organ size control, tissue homeostasis, and cancer. *Cell* 2015; **163**: 811–828.

14. Moroishi T, Hansen CG, Guan KL. The emerging roles of YAP and TAZ in cancer. *Nat Rev Cancer* 2015; **15**: 73–79.

15. Dong X, Meng L, Liu P, *et al*. YAP/TAZ: a promising target for squamous cell carcinoma treatment. *Cancer Manag Res* 2019; **11**: 6245–6252.

16. Wang Y, Dong Q, Zhang Q, *et al*. Overexpression of yes-associated protein contributes to progression and poor prognosis of non-small-cell lung cancer. *Cancer Sci* 2010; **101**: 1279–1285.

17. Saito H, Tenjin Y, Yamada T, *et al*. The role of YAP1 in small cell lung cancer. *Hum Cell* 2022; **35**: 628–638.

18. Ito T, Matsubara D, Tanaka I, *et al*. Loss of YAP1 defines neuroendocrine differentiation of lung tumors. *Cancer Sci* 2016; **107**: 1527–1538.

19. Baine MK, Hsieh MS, Lai WV, *et al*. SCLC subtypes defined by ASCL1, NEUROD1, POU2F3, and YAP1: a comprehensive Immunohistochemical and histopathologic characterization. *J Thorac Oncol* 2020; **15**: 1823–1835.

20. Minami K, Jimbo N, Tanaka Y, *et al*. Insulinoma-associated protein 1 is a prognostic biomarker in pulmonary high-grade neuroendocrine carcinoma. *J Surg Oncol* 2020; **122**: 243–253.

21. Rabban JT, Garg K, Ladwig NR, *et al*. Cytoplasmic pattern p53 immunoexpression in pelvic and endometrial carcinomas with TP53 mutation involving nuclear localization domains: an uncommon but potential diagnostic pitfall with clinical implications. *Am J Surg Pathol* 2021; **45**: 1441–1451.

22. Jimbo N, Ohbayashi C, Fujii T, *et al*. Implication of cytoplasmic p53 expression in pulmonary neuroendocrine carcinoma: analysis using next-generation sequencing. *Histopathology* 2024; **84**: 336–342.

23. Jimbo N, Ohbayashi C, Takeda M, *et al*. POU2F3-expressing small cell lung carcinoma and large cell neuroendocrine carcinoma show morphologic and phenotypic overlap. *Am J Surg Pathol* 2024; **48**: 4–15.

24. Kanda Y. Investigation of the freely-available easy-to-use software "EZR" (easy R) for medical statistics. *Bone Marrow Transplant* 2013; **48**: 452–458.

25. Yamatani C, Abe M, Shimoji M, *et al*. Pulmonary adenosquamous carcinoma with mucoepidermoid carcinoma-like component with characteristic p63 staining pattern: either a novel subtype originating from bronchial epithelium or variant mucoepidermoid carcinoma. *Lung Cancer* 2014; **84**: 45–50.

26. Babakoohi S, Fu P, Yang M, *et al*. Combined SCLC clinical and pathologic characteristics. *Clin Lung Cancer* 2013; **14**: 113–119.

27. Pelosi G, Fabbri A, Tamborini E, *et al*. Challenging lung carcinoma with coexistent DeltaNp63/p40 and thyroid transcription factor-1 labeling within the same individual tumor cells. *J Thorac Oncol* 2015; **10**: 1500–1502.

28. Hayashi T, Takamochi K, Yanai Y, *et al*. Non-small cell lung carcinoma with diffuse coexpression of thyroid transcription factor-1 and DeltaNp63/p40. *Hum Pathol* 2018; **78**: 177–181.

29. Savari O, Febres-Aldana C, Chang JC, *et al*. Non-small cell lung carcinomas with diffuse coexpressioclinic pathologicalclinico-pathological and genomic features of 14 rare biphenotypic tumours. *Histopathology* 2023; **82**: 242–253.

30. Quintanal-Villalonga A, Taniguchi H, Zhan YA, *et al*. Comprehensive molecular characterization of lung tumors implicates AKT and MYC signaling in adenocarcinoma to squamous cell transdifferentiation. *J Hematol Oncol* 2021; **14**: 170.

31. Hwang S, Hong TH, Kim HK, *et al*. Whole-section landscape analysis of molecular subtypes in curatively resected small cell lung cancer: clinicopathologic features and prognostic significance. *Mod Pathol* 2023; **36**: 100184.

32. Neptune ER, Podowski M, Calvi C, *et al*. Targeted disruption of NeuroD, a proneural basic helix-loop-helix factor, impairs distal lung formation and neuroendocrine morphology in the neonatal lung. *J Biol Chem* 2008; **283**: 21160–21169.

33. Huang YH, Klingbeil O, He XY, *et al*. POU2F3 is a master regulator of a tuft cell-like variant of small cell lung cancer. *Genes Dev* 2018; **32**: 915–928.

34. Ouadah Y, Rojas ER, Riordan DP, *et al*. Rare pulmonary neuroendocrine cells are stem cells regulated by Rb, p53, and Notch. *Cell* 2019; **179**: 403–416.e23.

35. Sutherland KD, Proost N, Brouns I, *et al*. Cell of origin of small cell lung cancer: inactivation of Trp53 and Rb1 in distinct cell types of adult mouse lung. *Cancer Cell* 2011; **19**: 754–764.

36. Ferone G, Lee MC, Sage J, *et al*. Cells of origin of lung cancers: lessons from mouse studies. *Genes Dev* 2020; **34**: 1017–1032.

37. Lim JS, Ibaseta A, Fischer MM, *et al*. Intratumoural heterogeneity generated by Notch signalling promotes small-cell lung cancer. *Nature* 2017; **545**: 360–364.

38. Rosen Y. Pulmonary neuroendocrine carcinomas in situ: do they exist? *Histopathology* 2022; **80**: 627–634.

39. Meder L, Konig K, Ozretic L, *et al*. NOTCH, ASCL1, p53 and RB alterations define an alternative pathway driving neuroendocrine and small cell lung carcinomas. *Int J Cancer* 2016; **138**: 927–938.

40. Lee JK, Lee J, Kim S, *et al*. Clonal history and genetic predictors of transformation into small-cell carcinomas from lung adenocarcinomas. *J Clin Oncol* 2017; **35**: 3065–3074.

41. Simbolo M, Centonze G, Ali G, *et al*. Integrative molecular analysis of combined small-cell lung carcinomas identifies major subtypes with different therapeutic opportunities. *ESMO Open* 2022; **7**: 100308.

SUPPLEMENTARY MATERIAL ONLINE

Figure S1. Pathological images of an old block and a recent block

Table S1. Details of the immunohistochemical protocols